Journal of Solid State Electrochemistry (2019) 23:1631–1640
https://doi.org/10.1007/s10008-019-04289-3

REVIEW PAPER

A comparative multiwavelength Raman spectroelectrochemical study of polyaniline: a review

Regina Mažeikienė[1] · Gediminas Niaura[1] · Albertas Malinauskas[1]

Received: 19 February 2019 / Revised: 23 April 2019 / Accepted: 24 April 2019 / Published online: 10 May 2019

Abstract

A comparative Raman spectroelectrochemical study on polyaniline electrodeposited at a gold electrode was performed within the broad range of spectra excitation wavelengths from UV (325 nm) through blue (442 nm), green (532 nm), red (633 nm) to NIR (785 nm) laser lines. Two solutions of pH 2.0 and 8.0 were selected for protonated and deprotonated forms of polyaniline, and two limiting redox forms, a reduced (leucoemeraldine), and a fully oxidized one were taken into account. Raman spectra obtained and discussed reveal a strong enhancement of spectra for reduced form at a short wavelength excitation, and for oxidized form at red and NIR excitations. Raman features for all four polyaniline forms differing in protonation degree and redox state were analyzed and compared; excitation wavelength-dependent characteristic marker bands were suggested.

Keywords Polyaniline · Raman spectroscopy · Spectroelectrochemistry · Multiwavelength · Redox processes

Introduction

Raman spectroscopy presents an exceptionally useful tool for elucidation of structure and properties of conducting and electroactive polymers deposited at a solid-liquid interface. In electrochemical systems, Raman spectroscopy enables to identify various forms of these materials differing in their oxidation and protonation degree, as well as to follow up interconversions between these forms. Some two decades ago, fundamental studies on Raman spectroscopy and spectroelectrochemistry of polyaniline and some of its derivatives were performed revealing distinctive spectral features for different forms of this polymer [1–6].

In general, three redox forms of polyaniline are usually distinguished—leucoemeraldine (reduced), emeraldine (half-oxidized), and pernigraniline (fully oxidized). At least the two first of them are known to be able to protonation in acidic solutions. These polyaniline forms differ in their light absorption properties. The protonated reduced form appears slightly yellow in color and absorbs in near UV spectral range around 320 nm. Upon a partial oxidation to the conducting emeraldine form, and a following full oxidation into pernigraniline form, the polymer turns bluish-green and deep blue, respectively, meaning a gradual increase in light absorbance in the red range of visible spectrum with the maximum beyond 600 nm. Also, an intermediate absorbance maximum around 420 nm could be observed at intermediate oxidation state [7]. Therefore, some of different laser lines used for exciting of Raman spectra could fall into a resonance with definite forms of this polymer. As a result, differently excited Raman spectra could differ drastically for the same redox form of this polymer. It is well-known that the use of blue excitation at 457 nm yields spectra of the reduced form of this polymer that are almost not sensitive to oxidation of polyaniline as well as to its protonation state [1]. This means that neither the different redox forms nor the electrochemically induced redox transformations could be studied with the use of blue laser line excitation. As opposite, the blue colored oxidized forms appear to be in a strong resonance with near infrared (NIR) (1064 nm) excitation, yielding rich in features spectra of these species [1]. The use of somewhat different excitation wavelengths also results in a similar behavior. Again, the insensitivity of spectra to the degree of protonation and oxidation was noted at blue excitation at 458 nm, whereas strong resonance for blue colored oxidized forms at a red (676 nm) and NIR (1064 nm) was observed [2, 3]. In contrast, the excitation within the middle range of visible spectrum at 488 nm and especially at 514 nm enables to observe all redox forms as

✉ Albertas Malinauskas
albertas.malinauskas@ftmc.lt

[1] Department of Organic Chemistry, Center for Physical Sciences and Technology, Sauletekio av. 3, 10257 Vilnius, Lithuania

well as their interconversions with the gradual shift of electrode potential [2]. Indeed, the green line excitation was accepted as best suited in the study of redox transformations and protonation effects of this polymer.

By using green (532 nm) excitation, we performed a detailed spectroelectrochemical study of polyaniline at different electrode potentials and different solution acidity [8]. Different redox forms were identified and characterized, and gradual reversible spectral changes were found to proceed by shifting the electrode potential within the limits used, thus showing probably the continuum in changes of the redox state of polyaniline driven by electrooxidation rather than the existence of the three "classic" redox states. Later, we studied electrochemically driven Raman spectra of polyaniline within a broad range of excitation wavelengths ranging from UV to NIR laser lines [9, 10]. In the present work, based on our comparative Raman spectroelectrochemical studies, we review Raman spectral features for two limiting forms of polyaniline—a reduced and a fully oxidized—at the two protonation levels—a protonated and a fully deprotonated—within a broad range of spectra excitation wavelengths ranging from UV to NIR laser lines.

Experimental details

In order to review Raman spectral features for the four selected forms of polyaniline at different spectra excitation laser line wavelengths, it is of primary importance to perform this comparative study under closely related conditions, keeping as far as possible many experimental variables constant, like electrode material and configuration used, the preparation procedures for electrode, electrodeposition of polyaniline layer, the configuration of electrochemical cell, the geometry of spectra excitation, and collection of scattered light. At the same time, the experimental set used should enable to change the laser excitation, electrolyte solutions, and electrochemical potential in a way not disturbing an overall experimental layout. Therefore, definite experimental conditions were applied as described below.

A cylinder-shaped electrochemical cell has been used in spectroelectrochemical experiments. As a working electrode, gold electrode of 5 mm in diameter, press-fitted into a Teflon rod holder and placed at about 2 mm distance from the cell optical window, was used. To reduce possible laser-induced thermo- and photoeffects, and a decomposition of polyaniline layer by laser beam as well, the cell has been continuously periodically moved with respect to laser beam at a rate of 15–25 mm s^{-1} using a custom built equipment, described in detail in [11, 12], and used in most of our works dealing with labile organic layers covered at an electrode surface. As a counter and reference electrode, platinum wire and saturated Ag/AgCl electrode were used, respectively. All electrode potential values given below refer to this reference electrode. For each experimental set, the working gold electrode was cleaned with a Piranha solution (a mixture of 30% hydrogen peroxide solution and concentrated sulfuric acid, 1:3 by volume) and then ultrasonicated in water-ethanol solution for 30 s. Throughout the work, a BASi-Epsilon model (Bioanalytical systems Inc., USA) potentiostat was used.

Polyaniline layer has been deposited on the working electrode in a separate electrochemical cell from a solution of 0.05 M of aniline in 0.5 M sulfuric acid. In order to get a uniform structure of polyaniline layer, electropolymerisation has been performed at mild conditions by applying a controlled potential of 0.8 V for 20 min. After that, the electrode was carefully rinsed and placed into spectroelectrochemical cell. As a working electrolyte, Britton-Robinson buffer solutions of pH 2.0 or 8.0, containing 0.1 M of potassium chloride, were used.

Raman spectra were recorded with a confocal microspectrometer inVia (Renishaw, UK) equipped with thermoelectrically cooled at − 70 °C CCD camera and microscope. For excitation of Raman spectra, the following lasers were used: a continuous-wave 325 nm (He-Cd laser 1 mW, 2400 lines mm^{-1} grating, spectral slit width 9.2 cm^{-1}), 442 nm (He-Cd laser 4 mW, 2400 lines mm^{-1} grating, spectral slit width 4.5 cm^{-1}), 532 nm (diode-pumped solid state laser 3 mW, 1800 lines mm^{-1} grating, spectral slit width 6.7 cm^{-1}), 632.8 nm (He-Ne laser 1 mW, 1200 lines mm^{-1} grating, spectral slit width 5.4 cm^{-1}), and 785 nm (diode laser 4 mW, 1200 lines mm^{-1} grating, spectral slit width 4.1 cm^{-1}). The spectral slit width values were determined from full width at half maximum (FWHM) of air O_2 band near 1555 cm^{-1}. The × 5/0.12 NA objective lens was used for excitation and collection of Raman spectra excited with all visible and NIR laser lines, and × 15/0.32 NA objective lens was used for UV laser line excited spectra.

Different structures of polyaniline

Electrodeposited layer of polyaniline can exist in several different forms depending on electrode potential and solution pH. Figure 1 displays six main forms of polyaniline. The first one is a reduced and non-protonated leucoemeraldine base (LB) form that exist at a low electrode potential in pH neutral or alkaline solutions. At pH under 3, protonation of this form proceeds leading to leucoemeraldine salt (LES) form, in which each second nitrogen atom becomes protonated. As for Raman spectroscopy, it is essential that both these reduced forms contain only benzene-type aromatic rings, without the presence of quinoid-type rings in their regular structure. By the positive electrode potential shift, two consecutive oxidation steps proceed. As obtained from cyclic voltammetry, the midpoint potentials for these two reversible redox steps are

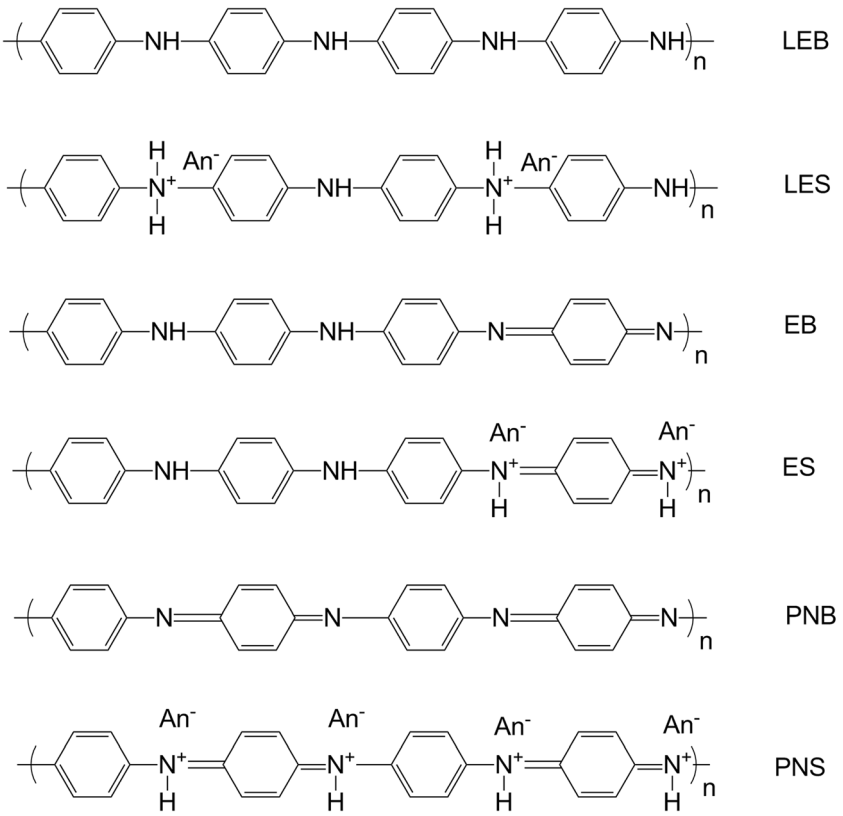

Fig. 1 Structures of the six main forms of polyaniline, taking into account their different redox forms and protonation levels. LEB leucoemeraldine base (reduced non-protonated form), LES leucoemeraldine salt (reduced protonated form), EB emeraldine base (half-oxidized non-protonated form), ES emeraldine salt (half-oxidized protonated form, here shown in its bipolaronic form), PNB pernigraniline base (fully oxidized non-protonated form), PNS pernigraniline salt (fully oxidized protonated form), An^- anion

located around 0.11–0.15 V and 0.75–0.80 V vs. Ag/AgCl reference in a solution of pH < 3, viz. for protonated forms of these species [13, 14]. At electrode potentials above the potential of the first redox transition, a semi-oxidized emeraldine form of polyaniline prevails. Again, depending on solution pH, a non-protonated emeraldine base (EB) form in pH-neutral or alkaline solutions, or a protonated emeraldine salt (ES) form in acidic solutions becomes prevailing. In both cases, it is essential for Raman analysis that both these half-oxidized emeraldine forms contain quinoid-type rings next to benzene-type ones. Considering the chemical structures (Fig. 1), the ratio of 3:1 of benzene to quinoid rings is characteristic for both these emeraldine forms. At the potentials more positive than the second redox step, the fully oxidized form of polyaniline, pernigraniline, appears most stable. Again, this one can exist either in a non-protonated pernigraniline base (PNB), or in a protonated pernigraniline salt (PNS) form depending on the solution acidity. Noteworthy, each second ring in a regular structure of PNB or PNS becomes quinoid, resulting in a 1:1 M ratio of benzoid and quinoid rings.

Different forms of polyaniline differ greatly in their light absorbance properties. For polyaniline deposited at a transparent ITO glass electrode, the absorbance spectra were presented in [7]. Figure 2 presents a derivative from those spectra showing the dependence in light absorbance on electrode potential, as calculated for specific wavelengths which correspond to laser lines used in excitation. The data presented in Fig. 2 allow to understand effects caused by the possible resonance enhancement of Raman spectra for specific excitation wavelengths, at least in acidic solutions. It is well seen that 325-nm excitation wavelength falls into a resonance with the reduced leucoemeraldine form that exist at low electrode potential; thus, characteristic features for this form of polyaniline are well observed and appear dominating over those of emeraldine and pernigraniline forms. For 442-nm excitation, an absorbance maximum around 0.2 V is observed (Fig. 2). This one corresponds to an intermediate redox form observed at this potential, as discussed in [9]. Because of a possible resonance, an increased Raman intensity has been noted and discussed at these intermediate potential values [9]. The lowest optical absorbance is observed at 532 nm. Accordingly, the 532-nm excitation allows one to observe all possible redox forms of polyaniline, thus making this excitation the most universal and useful in elucidation of spectral changes occuring upon electrochemical oxidation and reduction. The optical absorbance of polyaniline greatly increase with a positive potential shift in the red range of visible spectrum, causing the deep green-blue visible colouration of polyaniline film in contrast to pale yellow color characteristic for the reduced form. Accordingly, a steep increase in absorbance proceeds upon oxidation with 633 nm and especially 785-nm laser lines (Fig. 2). Accordingly, strong resonance is observed for emeraldine and pernigraniline forms at these red and especially NIR laser line excitations.

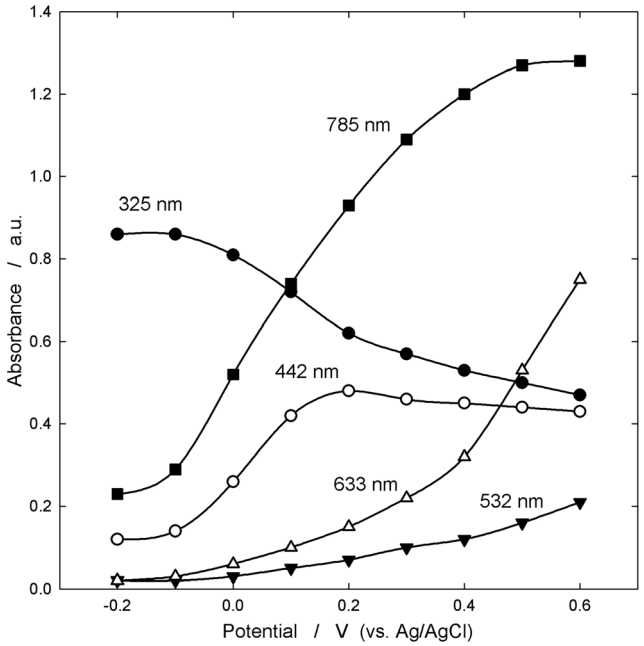

Fig. 2 Dependence of light absorbance on electrode potential for polyaniline electrodeposited at ITO electrode in solution of 0.5 M of sulfuric acid for laser line wavelengths used for excitation of Raman spectra (as indicated). The basic data have been taken from the spectra presented in [7], and recalculated for specific wavelengths and electrode potentials

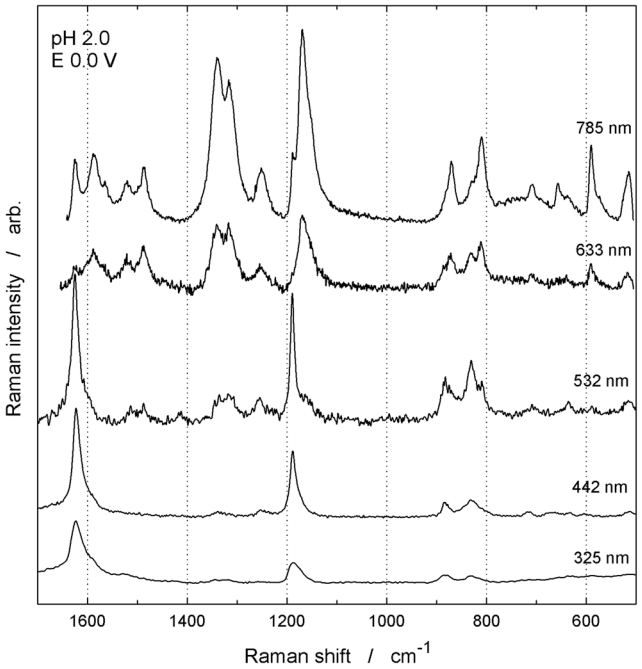

Fig. 3 Raman spectra of polyaniline layer at a gold electrode, as obtained in pH 2.0 solution at electrode potential of 0.0 V with different wavelengths of laser line excitation (as indicated)

Protonated reduced form of polyaniline

Figure 3 shows multiwavelength laser lines excited Raman spectra for the reduced and protonated form of polyaniline (i.e., protonated or proton-doped leucoemeraldine salt form, LES) in pH 2.0 solution at electrode potential of 0.0 V. As it could be expected, well-defined Raman band located around 1623–1625 cm^{-1} is observed, corresponding to C–C stretching vibrations in benzene rings, and thus characteristic for leucoemeraldine form of the polymer. At UV, blue, and green laser line excitations, this band appears strong to very strong in intensity and becomes dominating throughout an entire spectrum. For the red and NIR laser line excitations, however, this band appears less intense (Fig. 3). At the same time, a second characteristic Raman band within this wavelength range, centered around 1589 cm^{-1}, appears evident for red and NIR laser lines excitations. At a green, blue, and UV excitations, however, this Raman band appears either nearly undetectable or as a shoulder of a very low intensity near of the main 1625-cm^{-1} band.

These differences could be well understood taking into account specific UV-Vis light absorbance properties of different polyaniline forms. For LES form, the dominating absorbance band centered around 315 nm is well observed at a transparent ITO glass electrode [7]. As it follows from dependence of optical absorbance on electrode potential presented in Fig. 2, the 325-nm laser line used in the present work appears to be in a strong resonance with this UV light absorbance; therefore, striking features of this LES form are observed in the resulting spectrum. Same features are observed with the blue (442 nm), and green (532 nm) laser light excitations as well (Fig. 3). Just in the first works on Raman spectroscopy of polyaniline, it was found that the blue laser excitation line used (457 nm) yields Raman spectra of the reduced form of this polymer and does not show remarkable sensitivity to oxidation and protonation degree [1]. By the progressive oxidation of LES form to ES and PNS forms, new absorbance bands appear [7]. Among them, an intermediate band centered around 420 nm, corresponding probably to radical cations or isolated polarons generated in the course of a progressing oxidation, and a broad band or a series of bands above 600 nm, corresponding to localized and delocalized polarons, appear evident [7]. For this variety of absorbance bands, attempts have long been made to identify the corresponding redox forms of polyaniline by their characteristic bands [15]. Three main forms have been identified by a combined simultaneous UV-Vis and electron spin resonance study [16, 17]. An interesting attempt has been made by separating these complex bands into separate components, and ascribing them to different species generated during reversible oxidation and reduction of polyaniline [18, 19]. The presence of absorbance bands in the red range of spectrum, characteristic for the oxidized forms of polyaniline like ES and PNS, causes strong resonance Raman enhancement by using red, far red, and NIR laser line excitation. It is well seen from Fig. 2 that the optical absorbance grows greatly by exposing the

electrode potentials towards higher values for 633 nm, and especially for 785 nm excitation. Along with the insensitivity of Raman spectra to the degree of oxidation observed at a blue line excitation, a strong enhancement of Raman spectra due to presence of the blue-colored oxidized species was observed at NIR laser line (1064 nm) excitation [1]. Strong resonance for oxidized forms at the red (676 nm) and NIR (1064 nm) was noted [2, 3]. Because of a strong resonance, even the band centered around 1589 cm^{-1}, corresponding to C=C stretching vibrations in quinone-type rings, and thus characteristic for an oxidized form(s) of polyaniline, was observed at a red (633 nm) and NIR (785 nm) laser line excitation (Fig. 3), despite that this form should present in a very minor amount at the conditions indicated for Fig. 3 (0.0 V at pH 2.0). In summary, as a result of resonance, the 1625-cm^{-1} band appears strong or very strong at UV, blue, and green laser line excitation, and weak or mid-intense at a red and NIR excitation, whereas the 1589-cm^{-1} band, adversely, appears mid-intense or strong at the red and NIR excitation, correspondingly, and near undetectable at all three other excitation wavelengths. Assignments of the bands based on previous extensive resonance Raman studies of various polyaniline forms [1–6, 8, 20–30] along with the characteristic frequencies are listed in Table 1.

Another striking feature indicating reduced LES or oxidized ES or PNS forms is a C–H bending vibration band. The position of this band differs to somewhat extent depending on the oxidation state. For UV, blue, and green line excitation, this second-intense band, corresponding to leucoemeraldine redox state, appears around 1190–1188 cm^{-1}, whereas only shoulders can be observed at red and NIR laser line excited Raman spectra (Fig. 3). As opposite, another very intense C–H bending vibration band located at somewhat lower frequencies around 1170–1168 cm^{-1} is observed at a red and NIR excitation, characteristic for emeraldine redox state (Fig. 3). Here, the tendencies are the same as for a 1625–1589 cm^{-1} band couple: well expressed (obviously, due to resonance enhancement) leucoemeraldine C–H bending bands for UV to green laser line excitation, and strong emeraldine C–H bending band for green and NIR enhancement, most probably due to resonance enhancement of some residual amount of oxidized form present in a bulk of polyaniline layer.

Characteristic spectral features should be noted within the range of single and double C–N bonds stretching vibrations. The intensity of these bands varies from strong at NIR and red excitation to mid-intense or even weak for green and blue excitations, whereas no bands are observed at UV excitation (Fig. 3). For a single C–N bond, Raman band centered around 1254–1252 cm^{-1} is well observed, especially at NIR excitation (Fig. 3). Previously it was discussed that two amine group-related bands can be distiguished in Raman spectra at 1225 and 1255 cm^{-1} [23, 26, 27]. The lower frequency component was characteristic to base forms of polymer, while the higher frequency band was associated with salt form. Our data suggest that protonation of single carbon-nitrogen bond ($C–N^+$) is required for observation of this mode. Thus, the 1254–1252-cm^{-1} band was characteristic for the charged lattice observed only for LES form and was not visible for other forms.

A strong band around 1488–1486 cm^{-1} appears as a feature of a double C=N bond. This double bond belongs to oxidized forms of polyaniline like EB or ES in Fig. 1, probably present in residual quantity at a controlled potential of 0.0 V, and thus undergoing resonance enhancement at a red excitation. The most striking features are observed within the spectral range of 1400–1300 cm^{-1}. Here, C–N bands intermediate between a single and a double are evident. These bands belong to localized and delocalized polarons that causes conducting or semiconducting properties of polyaniline. Previously, we discussed the nature of these bands as studied by NIR laser excitation at 1064 nm [20]. As it could be expected, strong or very strong bands centered around 1341–1340 cm^{-1} and 1316 cm^{-1} were observed at NIR and red laser line excitation (Fig. 3). These two bands belong probably to the two kinds of polarons that differ in their localization degree, as we discussed previously [20]. At a green excitation, these bands merge into a complex mid-intense couple of bands within the range of 1340–1320 cm^{-1}, whereas spectra excitation at shorter wavelengths results in low-intense or even hardly detectable bands.

Next to these three Raman frequency ranges, where most striking changes proceed with varying of spectra excitation wavelengths, a number of other Raman bands are observed within the frequency range below 900 cm^{-1}. These are mostly weak to mid-intense, and expressed somewhat better for longer wavelength excitation, although even at UV excitation, some of them are well distinguishable (Fig. 3). These minor bands are summarized and tentatively ascribed in Table 1.

Protonated oxidized form

Upon shifting the electrode potential to higher values, oxidation of a polyaniline layer proceeds, resulting in essential changes in its structure. As an endpoint potential for pH 2.0 solution, we have chosen 0.8 V. This potential corresponds to the second oxidation step; thus, a fully oxidized protonated pernigraniline salt form (PNS), along with a half-oxidized protonated emeraldine salt form (ES), should prevail. Figure 2 shows a steep increase of optical absorbance by electrooxidation of polyaniline layer for red and especially NIR laser lines; thus, a strong resonance enhancement of Raman spectra is observed. To ensure full oxidation of polyaniline layer, even higher electrode potentials could be applied; however, this would lead to a remarkable degradation

Table 1 Characterization of Raman bands of polyaniline layer in reduced and oxidized forms deposited at a gold electrode, as obtained at different spectra excitation laser line wavelengths in pH 2.0 and pH 8.0 solutions at electrode potential of 0.0 V and 0.8 V

Solution pH	Raman bands (in cm^{-1}) for different redox forms of polyaniline and excitation wavelengths										Tentative assignments
	Reduced form					Oxidized form					
	785 nm	633 nm	532 nm	442 nm	325 nm	785 nm	633 nm	532 nm	442 nm	325 nm	
2.0	1625(m)	1625(w)	1625(vs)	1623(vs)	1624(s)	1620(w)	1623(m)	1623(m)	1620(s)	1623(vs)	C–C stretching in B (8a)
8.0	1610(vs)	1614(s)	1618(s)	1618(s)	1623(s)	–	1615(sh)	1616(m)	1619(s)	1621(vs)	
2.0	1589(s)	1589(m)	–	–	–	1583(s)	1585(s)	1583(s)	1584(m)	–	C=C stretching in Q (8a)
8.0	1591(sh)	1594(m)	1593(m)	–		1599(s)	1593(s)	1588(s)	1585(m)	–	
2.0	–	–	–	–	–	1554(w)	1555(w)	1553(m)	1551(m)	1555(w)	–
8.0	–	–	–	–	–	–	1554(w)	1545(w)	–	–	
2.0	1521(m)	1522(m)	1514(w)	–	–	–	–	–	–	–	–
2.0	1486(m)	1488(m)	1487(w)	–	–	1460(vs)	1471(vs)	1453(vs)	1465(vs)	1485(vs)	C=N stretching in emeraldine
8.0	1443(s)	1460(vs)	1444(s)	–	–	1454(vs)	1464(vs)	1461(vs)	1466(m)	1510(s)	base (imine sites)
2.0	–	–	–	–	–	1414(s)	1421(w)	1415(w)	1416(w)	1420(w)	–
8.0	1418(s)	–	–	–	–	1423(sh)	1428(sh)	1427(w)	1423(sh)	–	
2.0	–	–	–	–	–	1380(w)	1385(w)	1382(w)	–	–	C~N^+ stretching in polaronic
2.0	1340(vs)	1341(vs)	1343(m)	1339(vw)	–	1329(m)	1325(w)	1324(m)	1323(w)	1329(w)	form (polarons)
8.0	1334(m)	1331(m)	1330(m)	–	–	1318(w)	1321(w)	1321(m)	1322(w)	–	
2.0	1316(s)	1316(s)	1320(m)	–	–	–	–	–	–	–	
2.0	1252(s)	1253(m)	1255(w)	1254(w)	–	1223(s)	1221(s)	1223(s)	1223(s)	1224(m)	C–N stretching in emeraldine
8.0	1225(m)	1222(m)	1221(m)	–	–	1221(s)	1220(m)	1220(m)	1217(m)	1224(w)	(amine sites)
2.0	1189(sh)	–	1190(s)	1189(s)	1188(s)	–	–	–	–	–	C–H bending in
8.0	–	–	–	1181(m)	1182(m)	–	–	–	–	–	leucoemeraldine (9a)
2.0	1168(vs)	1170(s)	–	–	–	1161(vs)	1162(vs)	1161(vs)	1160(s)	1167(s)	C–H bending in emeraldine
8.0	1160(vs)	1162(s)	1161(s)	–	–	1162(vs)	1164(vs)	1162(s)	1164(s)	1176(m)	(9a)
2.0	872(m)	873(s)	884(m)	884(m)	883(m)	858(m)	851(w)	847(m)	–	879(m)	B deformation (1)
8.0	–	–	–	–	–	845(m)	842(w)	841(w)	–	–	
2.0	829(sh)	831(m)	830(s)	832(s)	830(m)	–	–	–	–	–	–
8.0	838(w)	839(w)	–	–	–	–	–	–	–	–	
2.0	–	812(m)	808(w)	–	–	800(s)	811(m)	–	–	–	C–N–C bending
8.0	809(w)	808(vw)	808(w)	–	–	–	–	–	–	–	
2.0	–	–	–	–	–	779(s)	777(s)	789(m)	–	–	Q deformation
8.0	782(w)	780(w)	778(w)	–	–	783(m)	779(m)	778(m)	785(m)	790(w)	
2.0	–	–	–	–	–	753(m)	754(m)	751(w)	–	–	Imine deformation (C–N–C
8.0	744(w)	747(w)	746(vw)	–	–	747(m)	749(m)	748(w)	–	–	bending)
2.0	709(w)	–	707(w)	–	–	–	–	–	–	–	–
2.0	657(w)	–	–	–	–	–	–	654(w)	654(w)	–	Ring deformation (6b)
8.0	646(w)	–	–	–	–	646(w)	651(w)	644(w)	–	–	
2.0	590(m)	590(m)	589(vw)	–	–	–	–	–	–	–	Ring deformation (6b)
8.0	572(w)	582(w)	579(w)	–	–	–	–	–	–	–	
2.0	515(m)	515(m)	514(w)	–	–	520(m)	523(m)	522(m)	531(m)	530(w)	Amine in-plane deformation
8.0	526(m)	530(w)	525(w)	–	–	523(m)	528(m)	526(m)	533(m)	–	

Assignments are based mainly on the known data [1–6, 8, 20–30]. The numbers given in parentheses (1), (6b), (8a), and (9a) refer to Wilson's notation of aromatic species vibration modes. Spectra for the reduced form of polyaniline were obtained at a controlled electrode potential of 0.0 V for pH 2.0 solution, or − 0.3 V for pH 8.0 solution, and spectra for oxidized form were obtained at a controlled potential of 0.8 V for pH 2.0 solution, or 0.3 V for pH 8.0 solution

B benzene-type ring, *Q* quinone-type ring, *(vs)* very strong, *(s)* strong, *(m)* mid-intense, *(w)* weak, *(vw)* very weak, *(sh)* shoulder, ~ bond intermediate between a single and a double, − the band of very weak or even undetectable intensity

of polyaniline, even during a relatively short spectra recording procedure. A fast decomposition of this polymer at higher potentials, and a steep dependence of the decomposition rate on electrode potential, has been shown previously [13, 14, 31]. Multiwavelength Raman spectra obtained for electrode potential of 0.8 V are presented in Fig. 4, and the main Raman features are tentatively ascribed in Table 1.

Drastic changes in spectra upon oxidation proceed within the range of 1620–1580 cm^{-1}, where C–C bond stretchings in benzene and quinone rings are evident. Electrooxidation of LES form of polyaniline leads consecutively to ES and, finally, to PNS forms (Fig. 1), where each fourth or each second benzene ring turns into quinone ring, respectively. As a consequence, an intense Raman band around 1585–1583 cm^{-1} is observed for NIR, red, and green line excitations (Fig. 4). As it could be expected owing to resonance enhancement of Raman spectra for blue-colored oxidized form, the relative intensity of this band diminishes in the said order, whereas blue excitation results in a relatively low intensity of this band (Fig. 4). At the same time, UV excited spectra show almost no band related to quinone rings (Fig. 4). In this respect, the features of the oxidized form appear almost invisible for UV excitation of Raman spectra.

Somewhat different situation is observed for another well-known feature of oxidized form, located around 1480–1450 cm^{-1}, corresponding to C=N bond stretching vibrations, characteristic for imine sites in ES and PNS forms. In the case of a reduced form, these stretchings were observed as mid-intense bands around 1488–1486 cm^{-1} at NIR and red excitation only, probably due to resonance with a small amount of this form at a low electrode potential. It is very likely that even a small content of oxidized form causes a strong resonance with NIR and, at a lower degree, with the red line excitation because of a high optical absorbance at these wavelengths (Fig. 2). For oxidized form, present at a potential of 0.8 V, however, these stretchings appear as very intense bands within the range of 1485–1453 cm^{-1}. Even for this dominating band, a decrease in a relative intensity is observed by consecutive moving from NIR to UV excitation (Fig. 4). However, even at UV excitation, this band appears very intense.

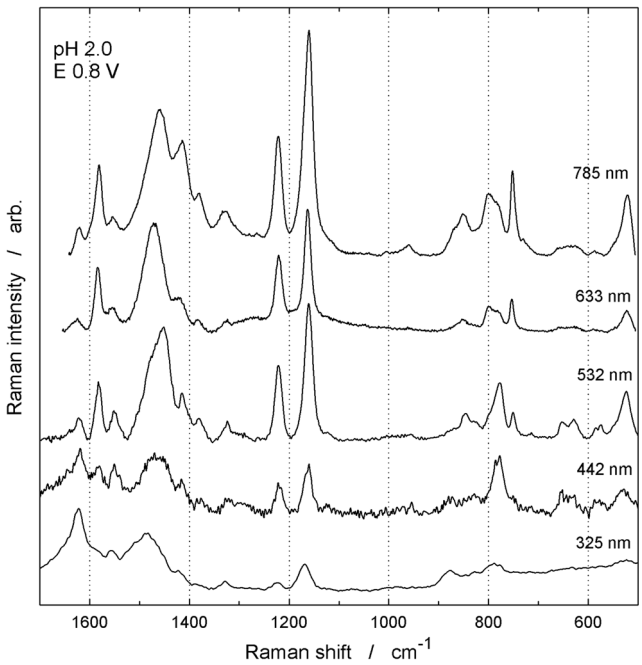

Fig. 4 Same as in Fig. 2, as obtained at electrode potential of 0.8 V

Another characteristic and strong band, well observed around 1224–1221 cm^{-1}, belongs to a single C–N bond stretching vibrations in emeraldine, i.e., to amine sites. Since it presents a feature of oxidized forms, its behavior again resembles that of C=N bond, as described above. The intensity of this band diminishes gradually by turning from NIR to UV excitation, although it remains quite intense even at UV excitation (Fig. 4). Important and well observable differences between the reduced and oxidized forms of polyaniline should be noted for C–H bending bands within their characteristic range of 1190–1160 cm^{-1}. As opposite to interplay between the two bands, observed at a low electrode potential, and ascribed to emeraldine and leucoemeraldine forms, as discussed above, the only strong or very strong band located around 1167–1160 cm^{-1} is observed, characteristic for C–H bending modes in oxidized ES and PNS forms (Fig. 4 and Table 1). The relative intensity of this band, again, diminishes gradually by turning from NIR to UV excitation.

Deprotonated reduced form

Figure 5 shows Raman spectra for polyaniline layer, as obtained at electrode potential of − 0.3 V in pH 8.0 solution. The main Raman features for deprotonated forms are collected and analyzed in Table 1. Under these conditions, polyaniline exist mainly in its non-protonated reduced form LEB. Within the range of C–C stretchings in B and Q rings, observed around 1600 cm^{-1}, again, an interplay between B and Q ring stretches could be observed depending on the excitation line used. For 325- and 442-nm excitations, a strong band around 1620 cm^{-1} could be observed. As distinct from acidic solution, the position of this band gradually shifts from 1623 to 1610 cm^{-1} by moving from UV to NIR laser excitation line. For protonated form, the position of this band remains almost independent on the excitation wavelength at 1624 cm^{-1}. We suggest that reason of such red shift is related with probing the more delocalized quinoid-type structures with 785-nm excitation. One can see appearance of strong lower frequency component of C=N stretching mode near 1418 cm^{-1} for this excitation wavelength; consequently, the benzenoid-type mode frequency downshifts to 1610 cm^{-1}. Such possibility was discussed by Folch et al. [28]; it was demonstrated that benzenoid ring stretching frequency (8a mode) decreases as delocalization of

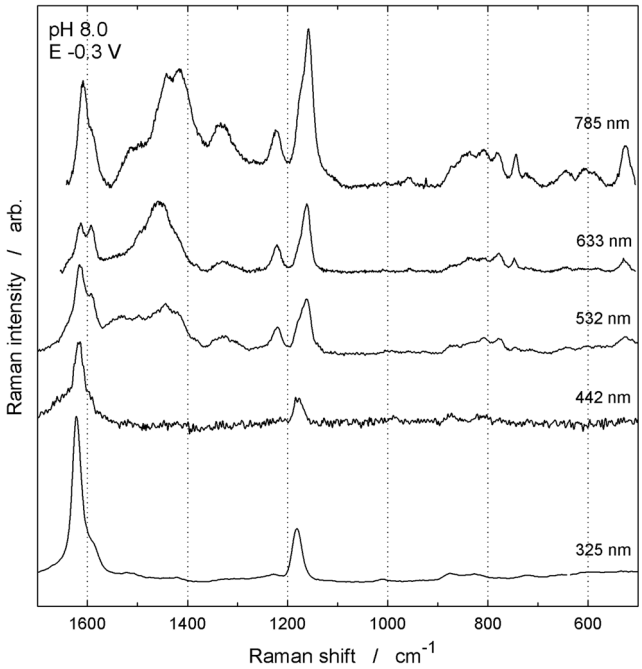

Fig. 5 Same as in Fig. 2, as obtained in pH 8.0 solution at electrode potential of − 0.3 V

polaronic structures increases. For the green laser line excitation, C=C stretches of Q rings become evident and develop into a well expressed band centered around 1594 cm^{-1} for 633 nm excitation (Fig. 5).

A similar interplay between C–H bending vibrations in leucoemeraldine and emeraldine forms is also well observable. For 325 and 442 nm excitations, a characteristic band for C–H bendings in LEB is observed centered around 1182–1181 cm^{-1} and thus shifted by 7–8 cm^{-1} to lower values, as compared to LES. This reflects protonation induced changes in leucomeraldine rings force constants; frequencies of both benzenoid ring C–C stretching (8a) and in-plane C–H bending (9a) vibrational modes upshift by 5–8 cm^{-1} (Table 1). It should be noted that LES form exhibits electronic transition near 315 nm [7] resulting in resonance enhancement of Raman modes coupled with this transition. For green, red, and NIR excitations, a strong band centered around 1162–1161 cm^{-1} is observed, corresponding to C–H bending vibrations in EB form. As compared to its protonated counterpart ES, this band appears shifted by approximately 7–9 cm^{-1} towards lower frequencies (cf. the corresponding data presented in Table 1).

It could be concluded that, similarly as for protonated forms, the appearance of Raman bands characteristic for C=C stretches in Q rings, and C–H bendings in EB form, as observed for pH 8.0 solution, indicates the presence of some amount of deprotonated oxidized form of polyaniline (EB or PNB) even at a low electrode potential of − 0.3 V, where the reduced form LEB should prevail.

One of the biggest differences between pH 2 and pH 8 solutions is that only mid-intense Raman band characteristic for intermediate (between a single and a double) C–N bond stretchings is observed for pH 8.0 at green, red, and NIR excitations within the range of 1350–1310 cm^{-1} (Fig. 5). In contrast, two strong or very strong Raman bands at 1340 cm^{-1} and 1316 cm^{-1} are observed in an acidic solution for red and NIR excitations (Fig. 3). This shows that protonation of polyaniline occurring at lower solution pH favors the development of polarons (charge carriers).

Another significant difference between these two solutions relates to C=N bond stretching vibrations. For pH 8.0 solution, strong to very strong Raman bands within the range of 1460–1443 cm^{-1} are observed, in contrast to weak or mid-intense bands around 1488–1486 cm^{-1}, observed in pH 2.0 solutions. This feature is best observed at red and NIR excitations, and belongs most probably to some amount of EB form present even at this low electrode potential.

Deprotonated oxidized form

Raman spectra for deprotonated oxidized form, designed as PNB in Fig. 1, relate to solution pH of 8, and electrode potential of 0.3 V. These conditions ensure nearly full conversion of polyaniline layer into its deprotonated oxidized form, retaining at the same time the relative stability of this material towards chemical decomposition, at least during the experiments. Figure 6 shows Raman spectra obtained at different excitation wavelengths, and the data thus obtained is summarized in Table 1. Again, an interplay between benzenoid and quinoid vibration modes around 1600 cm^{-1} is well seen. As it could be expected, UV excitation shows the only benzenoid band at 1621 cm^{-1}, whereas blue excitation results in a well expressed couple of benzenoid and quinoid bands, in contrast to deprotonated reduced form, for which this couple appears only for green excitation (cf. the corresponding spectra in Figs. 5 and 6). The green excitation, again, shows well expressed couple, whereas an approach or even merger of these bands appears for red and NIR excitation.

The characteristic C–H bending vibration in emeraldine form appears as a mid intense band at 1176 cm^{-1} for UV excitation and grows up to very intense band shifted to 1162 cm^{-1} for NIR excitation. Also, because the absence of leucoemeraldine form at this partial potential, no band centered around 1180 cm^{-1}, characteristic for C–H bending in leucoemeraldine form, is observed. In this respect, the deprotonated oxidized form shows closely similar features as the corresponding protonated form—the protonation does not influence these features.

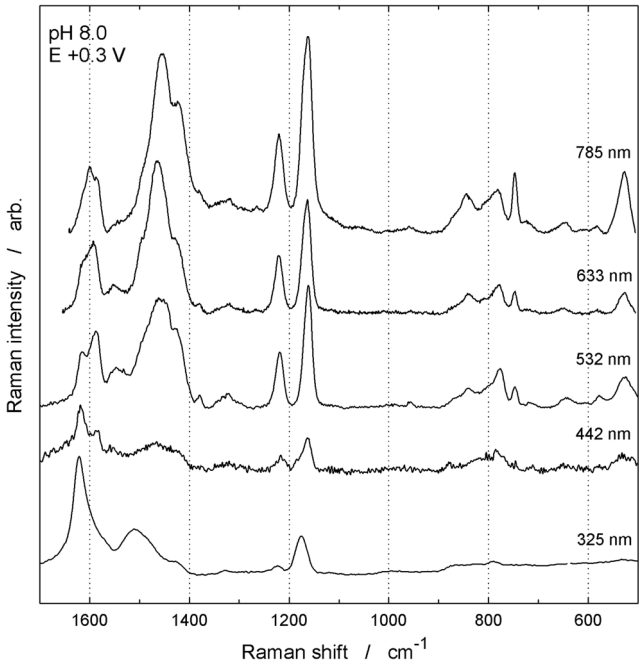

Fig. 6 Same as in Fig. 4, as obtained at electrode potential of 0.3 V

Although not well expressed, C~N^+ stretchings of polaronic form should be noted for green, red, and NIR excitations. Also, strong to very strong Raman bands, corresponding to C=N stretching in emeraldine base (imine sites), should be noted within the spectral range of 1510–1450 cm^{-1}. The intensity of this band grows up by moving to longer wavelength excitation; however, as opposed to deprotonated reduced form, this band is well observable even at UV and blue excitations. It should be noted that ν(C=N) band in UV excited spectrum is visible at higher frequency 1510 cm^{-1} comparing with VIS and NIR excitations (1454–1466 cm^{-1}) (Table 1). This might be an indication that UV excited spectrum probes less conjugated and stronger bonded C=N groups in PNB.

In common, both protonated and deprotonated oxidized forms gave similar Raman spectra. However, some differences between them should be noted. Perhaps the biggest visible difference taking place upon deprotonation, as it could be drawn from the data of (new version) Table 1, is the decrease in the wavenumber difference between the two prominent Raman bands which correspond to benzene- and quinone-type rings stretching vibrations (8a in Wilson's notation), well observable especially at longer wavelength excitations. For protonated oxidized polyaniline (at pH 2.0 and E 0.8 V), the said difference is 40 cm^{-1} and 38 cm^{-1} for 532-nm and 633-nm excitations, correspondingly, whereas for deprotonated oxidized form (at pH 8.0 and E 0.3 V), these differences are 28 cm^{-1} and 22 cm^{-1}, correspondingly. At a shorter wavelength excitation, this difference diminishes reaching 36 cm^{-1} and 34 cm^{-1} for protonated and deprotonated species, correspondingly, at a 442-nm excitation.

Conclusions

The present short review on a comparative spectroelectrochemical Raman study of polyaniline shows the crucial dependence of Raman spectra on excitation wavelengths used. At a UV (325 nm), and blue (442 nm) laser line excitation, the characteristic features of the reduced form are mostly observed, both for protonated (pH 2.0), and deprotonated (pH 8.0) forms of polyaniline. Even for oxidized species, the features of reduced form appear dominant. For UV excitation, almost no features of oxidized species could be observed, even at a high extent of polymer oxidation. Excitation at 442 nm provides possibility for sensitive probing protonation of leucoemeraldine chains; ring C–H bending frequency (9a) of LEB increases by 7–8 cm^{-1} and appears in LES at 1190–1188 cm^{-1}. It was found that 325-nm excited spectra probes less conjugated and stronger bonded C=N groups in PNB form of polymer.

Shifting the excitation line towards the longer wavelengths results in appearance of feature characteristic for oxidized form. Even for reduced form of polyaniline, the features of oxidized form, most probably present in minor quantities admixed to a bulk reduced form, are strongly evident, especially at a red (633 nm) and NIR (785 nm) excitations. The green laser line (532 nm) excitation appears most suited for spectroelectrochemical study, revealing both oxidized and reduced forms of polyaniline in its protonated and deprotonated forms. The appearance of C–N stretching band near 1254 cm^{-1} was found to be the characteristic marker for the presence of protonated single carbon-nitrogen bond network.

References

1. Lapkowski M, Berrada K, Quillard S, Louarn G, Lefrant S, Pron A (1995) Electrochemical oxidation of polyaniline in nonaqueous electrolytes: "in situ" Raman spectroscopic studies. Macromolecules 28(4):1233–1238
2. Quillard S, Berrada K, Louarn G, Lefrant S, Lapkowski M, Pron A (1995) In situ Raman spectroscopic studies of the electrochemical behavior of polyaniline. New J Chem 19:365–374
3. Lapkowski M, Berrada K, Quillard S, Louarn G, Lefrant S (1995) Study of the redox properties of polyaniline in non-aqueous media by Raman diffusion. J Chim Phys Phys-Chim Biol 92:915–918
4. Boyer M, Quillard S, Louarn G, Lefrant S, Rebourt E, Monkman AP (1997) Oxidized model compounds of polyaniline studied by resonance Raman spectroscopy. Synth Met 84(1-3):787–788
5. Bernard MC, Hugot-Le Goff A (1997) Raman spectroscopy for the study of polyaniline. Synth Met 85(1-3):1145–1146
6. Bernard MC, De Torresi SC, Hugot-Le Goff A (1999) In situ Raman study of sulfonate-doped polyaniline. Electrochim Acta 44(12):1989–1997
7. Malinauskas A, Holze R (1998) Cyclic UV-Vis spectrovoltammetry of polyaniline. Synth Met 97(1):31–36
8. Mažeikienė R, Tomkutė V, Kuodis Z, Niaura G, Malinauskas A (2007) Raman spectroelectrochemical study of polyaniline and

sulfonated polyaniline in solutions of different pH. Vib Spectrosc 44(2):201–208
9. Mažeikienė R, Niaura G, Malinauskas A (2018) Raman spectroelectrochemical study of polyaniline at UV, blue, and green laser line excitation in solutions of different pH. Synth Met 243:97–106
10. Mažeikienė R, Niaura G, Malinauskas A (2019) Red and NIR laser line excited Raman spectroscopy of polyaniline in electrochemical system. Synth Met 248:35–44
11. Niaura G, Gaigalas AK, Vilker VL (1997) Moving spectroelectrochemical cell for surface Raman spectroscopy. J Raman Spectrosc 28(12):1009–1011
12. Bulovas A, Dirvianskyte N, Talaikyte Z, Niaura G, Valentukonyte S, Butkus E, Razumas V (2006) Electrochemical and structural properties of self-assembled monolayers of 2-methyl-3-(ω-mercaptoalkyl)-1,4-naphthoquinones on gold. J Electroanal Chem 591(2):175–188
13. Mažeikienė R, Malinauskas A (2001) Kinetic study of the electrochemical degradation of polyaniline. Synth Met 123(2):349–354
14. Mažeikienė R, Malinauskas A (2002) Electrochemical stability of polyaniline. Eur Polym J 38(10):1947–1952
15. Stilwell DE, Park SM (1989) Electrochemistry of the conductive polymers. 5. In situ spectroelectrochemical studies of polyaniline films. J Electrochem Soc 136(2):427–433
16. Neudeck A, Petr A, Dunsch L (1999) Separation of the ultraviolet-visible spectra of the redox states of conducting polymers by simultaneous use of electron spin resonance and ultraviolet-visible spectroscopy. J Phys Chem B 103(6):912–919
17. Neudeck A, Petr A, Dunsch L (1999) The redox mechanism of polyaniline studied by simultaneous ESR-UV-vis spectroelectrochemistry. Synth Met 107(3):143–158
18. Nekrasov AA, Ivanov VF, Vannikov AV (2000) Analysis of the structure of polyaniline absorption spectra based on spectroelectrochemical data. J Electroanal Chem 482(1):11–17
19. Nekrasov AA, Ivanov VF, Vannikov AV (2001) Effect of pH on the structure of absorption spectra of highly protonated polyaniline analyzed by the Alentsev-Fock method. Electrochim Acta 46(26-27):4051–4056
20. Niaura G, Mažeikienė R, Malinauskas A (2004) Structural changes in conducting form of polyaniline upon ring sulfonation as deduced by near infrared resonance Raman spectroscopy. Synth Met 145(2-3):105–112
21. Da Silva JEP, De Torresi SIC, De Faria DLA, Temperini MLA (1999) Raman characterization of polyaniline induced conformational changes. Synth Met 101(1-3):834–835
22. Arsov LD, Plieth W, Kossmehl G (1998) Electrochemical and Raman spectroscopic study of polyaniline: influence of the potential on the degradation of polyaniline. J Solid State Electrochem 2(5):355–361
23. Louarn G, Lapkowski M, Quillard S, Pron A, Buisson JP, Lefrant S (1996) Vibrational properties of polyaniline – isotope effects. J Phys Chem 100(17):6998–7006
24. Baibarac M, Cochet M, Lapkowski M, Mihut L, Lefrant S, Baltog I (1998) SERS spectra of polyaniline thin films deposited on rough Ag, Au and Cu. Polymer film thickness and roughness parameter dependence of SERS spectra. Synth Met 96(1):63–70
25. Blomquist M, Lindfors T, Ivaska A (2007) Characterization of poly(N-alkylanilines) by Raman spectroscopy. Synth Met 157(22-23):974–983
26. Bernard MC, Hugot-Le Goff A (2006) Quantitative characterization of polyaniline films using Raman spectroscopy I: Polaronic lattice and bipolaron. Electrochim Acta 52:595–603
27. Cochet M, Louarn G, Quillard S, Buisson JP, Lefrant S (2000) Theoretical and experimental vibrational study of emeraldine in salt form. Part II. J Raman Spectrosc 31(12):1041–1049
28. Folch S, Gruger A, Regis A, Colomban P (1996) Optical and vibrational spectra of sols/solutions of polyaniline: water as secondary dopant. Synth Met 81(2-3):221–225
29. Trchová M, Morávková Z, Bláha M, Stejskal J (2014) Raman spectroscopy of polyaniline and oligoaniline thin films. Electrochim Acta 122:28–38
30. Ćirić-Marjanović G, Trchová M, Stejskal J (2008) The chemical oxidative polymerization of aniline in water: Raman spectroscopy. J Raman Spectrosc 39(10):1375–1387
31. Malinauskas A, Holze R (1999) In situ UV-Vis spectroelectrochemical study of polyaniline degradation. J Appl Polym Sci 73(2):287–294